

THE DOSE DEPENDENCE OF INERT GASES IRRADIATION HARDENING OF 316 AUSTENITIC STAINLESS STEEL AFTER LOW TEMPERATURE IRRADIATION

S.A. Karpov, G.D. Tolstolutskaia, V.N. Voyevodin, G.N. Tolmachova, I.E. Kopanets
Institute of Solid State Physics, Material Science and Technology NSC KIPT,
Kharkov, Ukraine
E-mail: karpofff@kipt.kharkov.ua

Irradiation-induced hardening has been investigated in relation to SS316 austenitic stainless steel. Samples were irradiated with 1400 keV/He and 1400 keV/Ar ions ions at fluences 0.01...10 displacements per atom (dpa) at room temperatures. Hardening of the surface layer was examined with nanoindentation. The behavior of the hardness-depth curve is analyzed with respect to the ion species. Regression analysis performed for hardening data using a power-law function of the form $\Delta H \propto (\text{dpa})^n$ gives good agreement with the experimental data at $n = 0.47$ and 0.13 for low-dose and high-dose hardening, respectively. An applying of volume fraction analytical model showed the possibility to simulate the hardness-depth behavior for ion-irradiated stainless steel with reasonable accuracy.

INTRODUCTION

Metals exposed to irradiation are known to harden due to the generation of Frenkel pair defect clusters that act as obstacles to dislocation motion under an applied stress. This hardening increases the yield strength, σ_y , of the material but reduces the ductility and causes embrittlement. Therefore characterizing the mechanical properties and quantifying the changes observed in the mechanical properties post irradiation is essential for the safe design of nuclear reactors.

Irradiation hardening in metallic materials is strong after irradiation at low temperatures (usually below 300 °C) because significant quantities of radiation-induced defect clusters are retained, and they impede the generation and glide of dislocations during deformation [1].

The effects of high levels of helium under conditions of simultaneous displacement damage production and irradiation embrittlement are two of the most important issues facing the development of steels for fusion applications [2].

The 300 series austenitic stainless steels provide high resistance to corrosion and oxidation and retain high strength and excellent ductility over a temperature range from cryogenic to elevated temperatures [3]. Such favorable properties enable those steels to meet requirements for application in nuclear facilities.

To simulate neutron irradiation damage of the structural materials, heavy ion irradiation experiments

have been used because of the simplicity of use, easier control of irradiation parameters, reduction of cost, rapid damage production, the absence of induced radioactivity, and the occurrence of the co-implantation of helium/hydrogen.

On the other hand, ion irradiation has a significant drawback – shallow depth of damage layer that making it difficult to investigate the mechanical properties. The solution of problem is possible by using nanoindentation method that provides a study of the mechanical properties of the samples in the near-surface region. However, for the successful implementation of this methodology, it is necessary to resolve such issues as the correlation the change in strength with the plastic deformation, the dose dependent of defect-cluster accumulation and the damage gradient effect.

The aim of the present work is the determine the dose dependent hardness from nanoindentation in heavy ions irradiated SS316 steel and investigation of effects of damage gradient and high levels of helium on the hardening of SS316 steel.

1. MATERIAL AND METHODS

The specimens of SS316 steel with dimensions 10×7×0.1 mm were used for investigations. Before experiments the samples were annealed at 1340 K for one hour in a vacuum $\sim 10^{-4}$ Pa. Chemical composition of steel is shown in Tabl. 1.

Table 1

Chemical composition of SS316 steel, wt.%

C	Si	Mn	P	S	Cr	Ni	Mo	Fe
< 0.080	< 0.75	< 2.0	< 0.045	< 0.030	17.5	13.1	2.3	balanced

Samples were irradiated with 1.4 MeV argon ions to a dose of $2.8 \cdot 10^{15} \text{ cm}^{-2}$ and 1.4 MeV helium ions to a dose of $8 \cdot 10^{17} \text{ cm}^{-2}$. All irradiations were carried out with accelerating-measuring system “ESU-2” [4]. The irradiation was performed at room temperature. Part of each sample was masked from the ion beam, allowing both an irradiated and unirradiated region of the sample to be examined post irradiation.

Studies of the steel microstructure were performed by transmission electron microscopy at room temperature, employing standard bright-field techniques on an EM-125 electron microscope at accelerating voltage 125 kV. Preparation of specimens to suitable for TEM thickness was performed using standard jet electropolishing from unirradiated surface. The initial structure of SS316 steel is shown in Fig. 1.

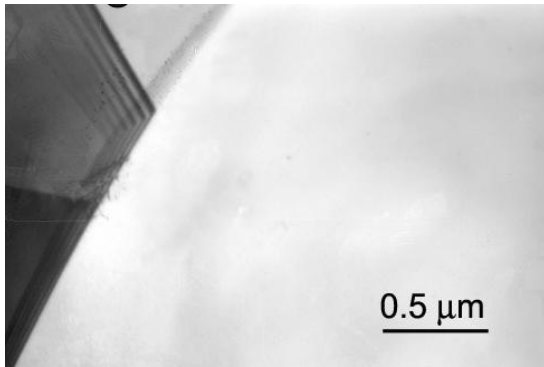


Fig. 1. The initial microstructure of SS316 steel after heat treatment at 1340 K/0.5 h

Nanohardness was measured by Nanoindenter G200 with a Berkovich type indentation tip. Tests were performed with a constant deformation rate of 0.05 s^{-1} . As a rule, ten measurements were performed every time at a distance of 35 μm from each other with subsequent averaging of the results.

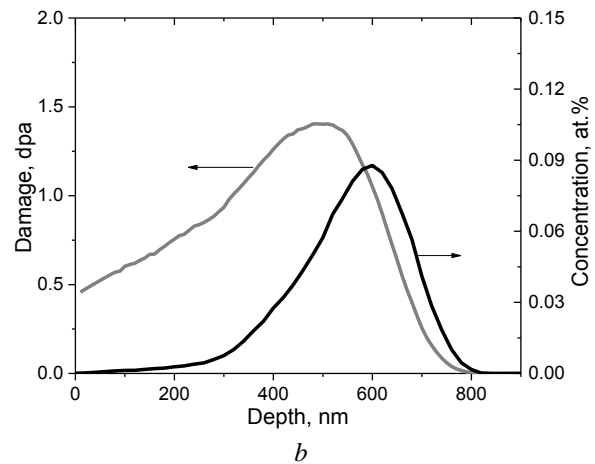
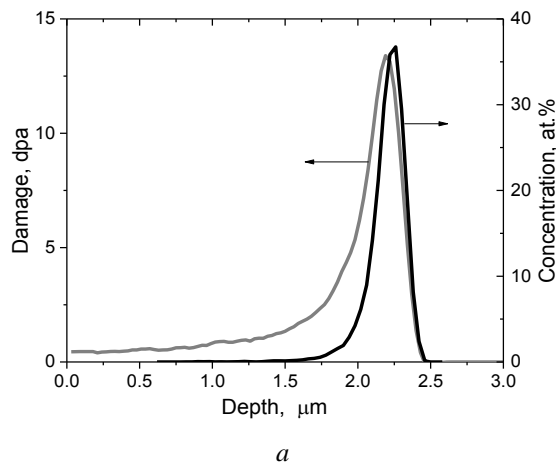


Fig. 2. Damages and concentrations profiles as a function of depth calculated using SRIM for 1400 keV He^+ (a) and 1400 keV Ar^+ (b)

Hardness (H) as a function of indenter displacement (h) is given in Fig. 3.

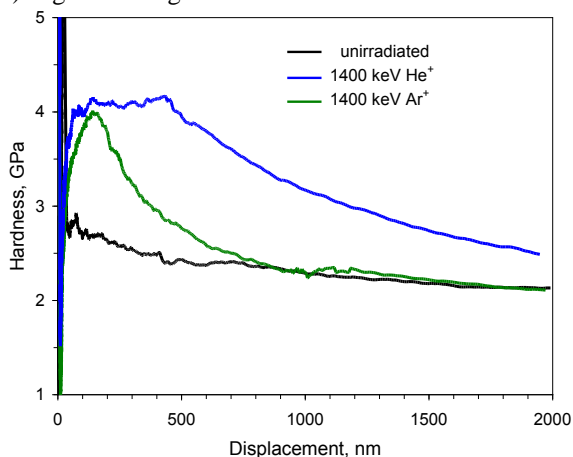


Fig. 3. Nanoindentation hardness of SS316 steel vs. indentation depth of the unirradiated sample and samples irradiated with He^+ and Ar^+ at T_{room}

In all samples, the first 100 nm of displacement shows a considerable increase in the scatter of the data

The methodology of Oliver and Pharr was used to find the hardness [5]. The details of nanoindentation tests have been presented elsewhere [6].

2. RESULTS AND DISCUSSION

In present paper we have determined values of nanohardness of SS316 steel in the initial state and after irradiation with 1.4 MeV helium or argon ions at T_{room} .

The depth distribution of gas atoms concentration and damage for ion irradiation with helium and argon ions shown in Fig. 2.

Ion stopping distribution for helium and argon ions and irradiation damages (in dpa) in stainless steel have been calculated with the software The Stopping and Range of Ions in Matter (SRIM 2008) [7]. The dpa calculations are based on a displacement energy threshold of 40 eV and on the Kinchin-Pease formalism and Stoller recommendations [8].

due to tip-rounding artifacts [9] and surface preparation effects. Therefore, for all samples the first 100 nm of data will be ignored for the remainder of the analysis.

After the ion irradiation of specimens with He and Ar ions at T_{room} an increase of nanohardness of about two times is observed, independently of species of ions.

Indentation of ion irradiated materials will give hardness that results from a superposition of the bulk hardness, indentation size effect and the irradiation induced hardening. The region of plastically deformed material beneath the indentation penetrates significantly deeper (Fig. 4) into the material than the displacement of the indenter. Previous studies have shown that the plastic zone can be approximated by a hemisphere with a radius of 5...10 times the indentation depth [1]. Therefore, in an irradiated material with a shallow damage depth, it is probable that part of the plastic zone will extend in the underlying, unirradiated material. With increasing of indentation depth, the measured hardness will approach the hardness of unirradiated material, since the part of unirradiated material within the plastic zone increases.

In accordance with this consistency, peaks at 150 and 400 nm contact depth in the hardness profile (see

Fig. 3) corresponded to a SRIM calculated peaks at 500 and 2200 nm for argon and helium, respectively.

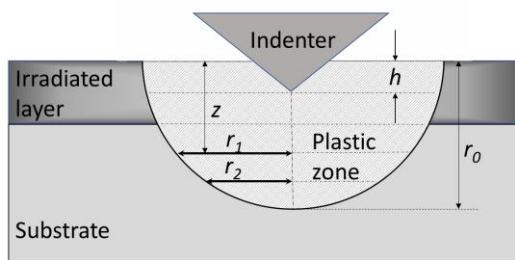


Fig. 4. Schematic of the indentation test. The indentation-induced plastic zone is assumed to be a hemisphere

The method of consideration of the soft substrate effect for materials irradiated with accelerated ions was first proposed by Kasada et al. in [10], where materials of this kind were considered as system with coatings or as “hardened layer–substrate” systems. The hardness of the ion-irradiated region, according to Kasada, can be determined by fitting the depth profile in the range of $100 \text{ nm} < h < h_c$ (h_c is critical indentation depth) to the Nix-Gao model [11].

By redrawing the experimental profiles of hardness (see Fig. 3) in the coordinates “squared hardness–reciprocal depth”, the bulk-equivalent hardness of the ion-irradiated region has been evaluated from the intercept of the linear fitting of data in the range of $100 \text{ nm} < h < 400 \text{ nm}$ for He-irradiated sample and in the range of $100 \text{ nm} < h < 150 \text{ nm}$ for the Ar-irradiated sample. The values of bulk-equivalent hardness were found to be 4.2 and 3.8 GPa for helium and argon irradiation, respectively.

2.1. THE DOSE DEPENDENCE OF IRRADIATION HARDENING

Ref. [12] represents our previous results of study of irradiation effect with 1.4 MeV argon ions within the range of doses 0...10 dpa at 300 K on the hardening of SS316 stainless steel. The hardness of the ion-irradiated region of material has been determined according to above mentioned approach of Kasada. It was discovered that the nanohardness of the steel increases with the damaging dose in the entire interval of radiation doses. The sharpest effect is observed at low doses with a gradual approach of the quasisaturation mode at high fluencies.

It should be noted that G.S. Was et al. analyzing the data of radiation induced segregation, irradiated microstructure, radiation hardening and IASCC susceptibility of the same heats of proton- and neutron-irradiated 304SS and 316SS have shown that the irradiation hardening of austenitic steels saturates at about a few dpa [13].

A great deal of effort has been made to explain the irradiation hardening behavior of metals, and to correlate the change in strength with the number density and size of radiation-induced defects and with irradiation dose. Although there are multiple hypotheses concerning the mechanisms of irradiation hardening [14], the dose-dependence of the increase in yield stress, $\Delta\sigma_{ys}$, has been explored frequently using models based on barrier hardening theory [15].

In the regression analysis [14], the radiation-induced increase in yield stress, $\Delta\sigma_{ys}$, was expressed in the form of a power law: $\Delta\sigma_{ys} = h \cdot (\text{dpa})^n$, where h and n are the regression coefficients and dpa is displacements per atom. The log-log plots of $\Delta\sigma_{ys}$ vs. dpa data showed two distinctive regimes: a low-dose regime where a rapid hardening occurs and a high-dose regime where the log-log plot shows a considerably reduced slope. Mean values for n obtained from the 19 metals were about 0.5 for the low-dose regime and about 0.12 for the high-dose regime.

The dose dependence of irradiation hardening in SS316 irradiated with 1.4 MeV Ar ions is seen in Fig. 5. The hardening data obtained in present study for helium and argon irradiation are also included.

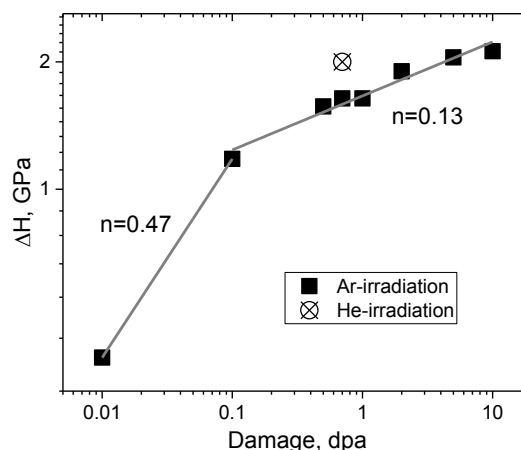


Fig. 5. Log-log plot for dose dependence of irradiation hardening of 316 stainless steels

Approximation of hardness values by a power function of the form $\Delta H \propto (\text{dpa})^n$ gives good agreement with the experimental data at $n = 0.47$ and 0.13 for low-dose and high-dose hardening, respectively.

In general n values were in the range 0.31...0.48 in the low-dose regime and 0.01...0.24 in the high-dose regime for the fcc metals; the average for the low-dose regime, 0.4, was slightly lower than that for bcc metals, 0.55 [1]. Also, a trend band for 316 stainless steels irradiated and tested at low temperatures ($\leq 110 \text{ }^\circ\text{C}$) was obtained from the database for 316 stainless steels [16] and shown that the n values for the database were 0.38 and 0.04 for the low-dose and high-dose regimes, respectively.

2.2. THE VOLUME FRACTION MODEL

The values of bulk-equivalent hardness discussed in previous paragraphs have been evaluated in accordance with the methodology of Kasada et al. [10] from the data fitting of the Nix-Gao plot. However, this method did not take into account the damage gradient effect (DGE). To extract irradiation induced hardening effect precisely with a consideration of DGE, a rule-of-mixtures type volume fraction approach has been used. This method has recently been described in [17–19].

In the framework of this approach, the hardness is a volume-weighted average of the hardness of plastically deformed material in the irradiated layer and the unirradiated underlying substrate. Since the hardness changes with the dose over the depth, the irradiated

layer can be divided into segments. Each segment is assigned to its dose-dependent hardness for further calculations of their individual contributions to the overall hardness. The method allows to distinguish the contribution of radiation hardening, ISE and substrate hardness to the measured hardness.

The volume fraction model includes the following assumptions:

1). The nanoindent is surrounded with a hemispherical plastic zone beneath the surface. The radius of hemisphere is larger than the indent depth by a certain factor. This factor was fixed at 7 for simplicity. It is assumed that the plastic zone increases linearly in radius with indent depth.

2). The plastic zone is divided into a number of segments with the same height $h = 20$ nm (see Fig. 4). For each indent depth, the plastic zone extended from the top surface to a certain depth, and each segment of the plastic zone contributed to the overall hardness measured at that indent depth. So that, for a maximum indent of 2000 nm, the whole calculation depth would be 14 μ m deep, and would contain 700 segments of 20 nm.

3). The volume of each segment is calculated for all segments within the plastic zone as

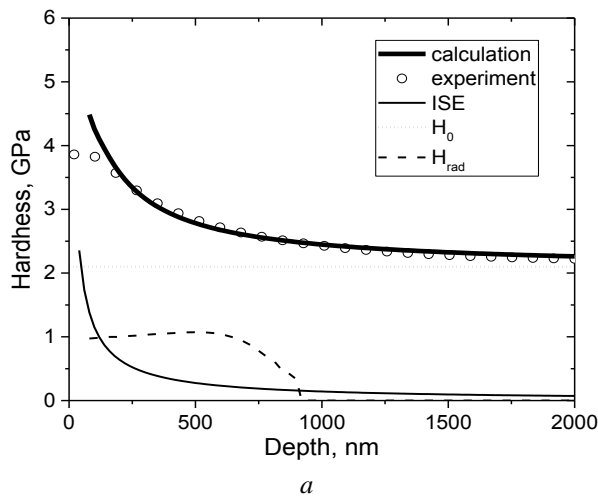
$$V = \frac{\pi h}{6} (3r_1^2 + 3r_2^2 + h^2), \quad (1)$$

where $r_1^2 = r_0^2 - z^2$, $r_2^2 = r_0^2 - (z+h)^2$, r_0 is the plastic zone radius at the current indentation depth and z (increases in increments of h depending on the segment number) is the depth of the top of the segment from the surface (see Fig. 4).

4). The radiation induced hardening of each segment was calculated according to the simple power law relationship as:

$$\Delta H_{rad} = m(D)^n, \quad (2)$$

where D is the dose in dpa and m and n are constants. The dose at each depth was taken from the SRIM calculations shown in Fig. 2.



5). According to volume fraction model, the calculated radiation induced hardness at each indent depth is the weighted average hardness of the segments in the plastic zone:

$$H_{rad} = \frac{\sum \Delta H_{rad(i)} \times V_{(i)}}{\sum V_{(i)}}, \quad (3)$$

where $\Delta H_{rad(i)}$ is the hardness value for segment i , and $V_{(i)}$ is the volume of segment i .

To simulate contact depth hardness H_C , we assume that H_C is a linear superposition of the hardness of the unirradiated substrate H_S and the irradiation-induced hardness H_{rad} .

$$H_C = H_S + H_{rad}. \quad (4)$$

The hardness of the unirradiated substrate H_S consists of the hardness due to the indentation size effect, H_{ISE} , and the material hardness at an infinite depth, H_0 .

$$H_S = H_{ISE} + H_0. \quad (5)$$

Assuming that H_{ISE} and H_0 are specific to the material, these can be used in Equation (4) to model the irradiated material. To obtain the Nix-Gao parameters H_0 and h^* (a characteristic length), an approach [12] have been applied to the unirradiated hardness data. The values of 2.1 GPa and 190 nm were found for H_0 and h^* , respectively.

The constants m and n are adjusted until agreement is reached between the experimental and calculated hardness vs. depth curves.

Fig. 6 shows the results of hardness-depth curve simulations as well as experimental data for the cases of argon and helium irradiation. The hardness H_{rad} obtained from the volume fraction model is given as dashed line. Parameters used in simulation are listed in Table 2.

Table 2

Simulation parameters		
Irradiation conditions	m	n
Ar	1	0.2
He	1.5	0.2

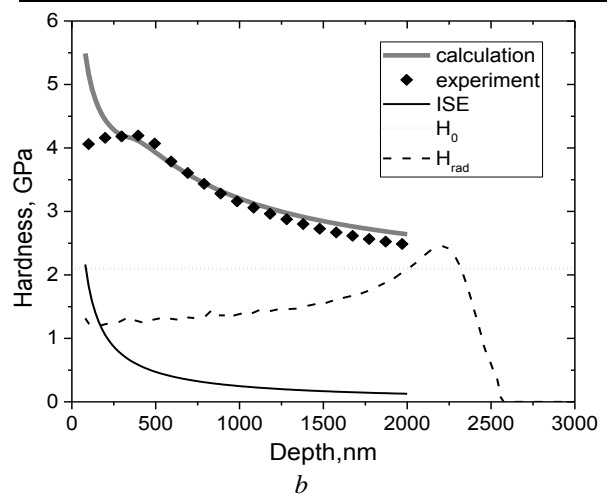


Fig. 6. Experimental hardness vs. displacement plot for 1.4 MeV Ar (O) (a) and 1.4 MeV He (\blacklozenge) (b). The bold solid black and gray lines show the hardness obtained from the volume fraction model. The dotted lines show the material hardness at an infinite depth H_0 ; fine black lines – ΔH_{ISE} vs. indenter displacement. The dashed lines show the irradiation-induced hardness H_{rad} vs. depth

It is seen that model exhibited good correlation, both qualitatively and quantitatively, to the experimental curves. The position, shape and calculated values of the hardness-depth plot for Ar-irradiated sample are close enough to the experimental results. For the case of He irradiation, a slight discrepancy is observed in the region of depths greater than 1500 nm. This may be caused by the fact that at this depth the layer of implanted helium ions arises (see Fig. 2) and reaches a concentration over 30 at.% at a depth of 2.2 μm . The presence of helium in such quantities can affect the hardness profile of irradiated steel.

It should also be noted that the value of the constant n correlates with the value of the exponent of the power function for the high-dose irradiation regime, which was discussed in paragraph 2.1.

The hardness depth profile after ion irradiation includes three different depth dependent effects: ISE, DGE and effect of substrate. Irradiation with gaseous (He, Ar) ions also should give additional effect in the implanted layer – implanted-ion effect. Although this effect is believed to be smaller than the effect of irradiation hardening due to displacement damage, it requires substantive consideration.

The data obtained in the present study indicate that a significant loss of ductility of the austenitic steels of 300 series will be expected at fluences about 1...5 dpa where the saturation of the density of the dislocation loops is observed, and the accumulation of He/H becomes significant.

CONCLUSIONS

Irradiation-hardening behaviors have been investigated for SS316 austenitic stainless steel after low-temperature ($< 100\text{ }^\circ\text{C}$) irradiations. The following conclusions were drawn:

The log-log plots of ΔH vs. dpa data showed two distinct regimes: a low-dose regime and a high-dose regime. Regression analysis performed for those regimes using a power-law function of the form $\Delta H \propto (\text{dpa})^n$ gives good agreement with the experimental data at $p = 0.47$ and 0.13 for low-dose and high-dose hardening, respectively.

The simple volume fraction analytical model demonstrated the ability to simulate the hardness-depth behavior for ion-irradiated stainless steel with reasonable accuracy. This allows to predict changes in hardness at a specified level of radiation damage.

REFERENCES

1. T.S. Byun, K. Farrell. Irradiation hardening behavior of polycrystalline metals after low temperature irradiation // *J. Nucl. Mater.* 2004, v. 326, p. 86-96.
2. T. Yamamoto, G. Robert Odette, H. Kishimoto, Jan-Willem Rensman, P. Miao. On the effects of irradiation and helium on the yield stress changes and hardening and non-hardening embrittlement of $\sim 8\text{ Cr}$ tempered martensitic steels: Compilation and analysis of existing data // *J. Nucl. Mater.* 2006, v. 356, p. 27-49.
3. В.Н. Воеводин, И.М. Неклюдов. *Эволюция структурно-фазового состояния и радиационная стойкость конструкционных материалов*. Киев: «Наукова думка», 2006, 376 с.
4. Г.Д. Толстолицкая, В.В. Ружицкий, И.Е. Копанец, В.Н. Воеводин, А.В. Никитин, С.А. Карпов, А.А. Макиенко, Т.М. Слюсаренко. Ускорительный комплекс для изучения поведения гелия и водорода в условиях генерации радиационных дефектов // *Problems of Atomic Science and Technology. Series "Physics of Radiation Effect and Radiation Materials Science"*. 2010, N 1, p. 135-140.
5. W.C. Oliver, G.M. Pharr. An improved technique for determining hardness and elastic modulus using load and displacement sensing indentation experiments // *J. Mater. Res.* 1992, v. 7, N 6, p. 1564-1583.
6. G.N. Tolmachova, G.D. Tolstolutskaya, S.A. Karpov, B.S. Sungurov, R.L. Vasilenko. Application of nanoindentation for investigation of radiation damage in SS316 stainless steel // *Problems of Atomic Science and Technology. Series "Physics of Radiation Effect and Radiation Materials Science"*. 2015, N 5(99), p. 168-173.
7. ASTM E521-96, 2009, ASTM.
8. <http://www.srim.org/>
9. Z. Xue, Y. Huang, K.C. Hwang, and M. Li. The influence of the indenter tip radius on the micro-indentation hardness // *J. Eng. Mater. Technol.* 2002, v. 124, p. 371-379.
10. R. Kasada et al. A new approach to evaluate irradiation hardening of ion-irradiated ferritic alloys by nano-indentation techniques // *Fusion Eng. Des.* 2011, v. 86, p. 2658-2661.
11. W.D. Nix, H.J. Gao. Indentation size effects in crystalline materials: A law for strain gradient plasticity // *J. Mech. Phys. Solid.* 1998, v. 46, p. 411-425.
12. S.A. Karpov, G.D. Tolstolutskaya, B.S. Sungurov, A.Yu. Rostova, G.N. Tolmacheva, I.E. Kopanets. Hardening of SS316 Stainless Steel Caused by the Irradiation with Argon Ions // *Materials Science*. 2016, v. 52, issue 3, p. 377-384.
13. G.S. Was et al. Emulation of neutron irradiation effects with protons: validation of principle // *Journal of Nuclear Materials*. 2002, v. 300, p. 198-216.
14. B.N. Singh, A.J.E. Foreman, H. Trinkaus. Radiation hardening revisited: role of intracascade clustering // *J. Nucl. Mater.* 1997, v. 249, p. 103-115.
15. A.F. Rowcliffe, S.J. Zinkle, J.F. Stubbins, D.J. Edwards, D.J. Alexander. Austenitic stainless steels and high strength copper alloys for fusion components // *J. Nucl. Mater.* 1998, v. 258-263, p. 183-191.
16. J.E. Pawel, A.F. Rowcliffe, D.J. Alexander, M.L. Grossbeck, K. Shiba. Effects of low temperature neutron irradiation on deformation behavior of austenitic stainless steels // *J. Nucl. Mater.* 1996, v. 233-237, p. 202-206.
17. P. Hosemann, D. Kiener, Y. Wang, S. Maloy. Issues to consider using nanoindentation on shallow ion beam irradiated materials // *J. Nucl. Mater.* 2012, v. 425 (1-3), p. 136-139.
18. H.-S. Kim et al. A novel way to estimate the nanoindentation hardness of only-irradiated layer and its application to ion irradiated Fe-12Cr alloy // *J. Nucl. Mater.* 2017, v. 487, p. 343-347.
19. M. Saleh et al. Relationship between damage and hardness profiles in ion irradiated SS316 using nanoindentation —experiments and modeling // *Int. J. Plast.* 2016, v. 86, p. 151-169.

Статья поступила в редакцию 31.08.2018 г.

ДОЗОВАЯ ЗАВИСИМОСТЬ УПРОЧНЕНИЯ 316 АУСТЕНИТНОЙ НЕРЖАВЕЮЩЕЙ СТАЛИ ПРИ НИЗКОТЕМПЕРАТУРНОМ ОБЛУЧЕНИИ ИОНАМИ ИНЕРТНЫХ ГАЗОВ

С.А. Карпов, Г.Д. Толстолицкая, В.Н. Воеводин, Г.Н. Толмачева, И.Е. Копанец

Изучено радиационно-индуцированное упрочнение аустенитной нержавеющей стали SS316. Образцы облучали ионами 1400 кэВ/He и 1400 кэВ/Ar до доз 0,01...10 смещений на атом (сна) при комнатной температуре. Упрочнение поверхностного слоя исследовали методом наноиндентирования. Проанализировано поведение кривой твердость–глубина в зависимости от сорта ионов. Регрессионный анализ, выполненный для данных по упрочнению с использованием степенной функции вида $\Delta H \propto (\text{сна})^n$, хорошо согласуется с экспериментальными данными при $n = 0,47$ и $0,13$ для низкодозного и высокодозного режимов упрочнения соответственно. Применение аналитической модели объемной доли показало возможность с достаточной точностью моделировать поведение твердости по глубине облученной нержавеющей стали.

ДОЗОВА ЗАЛЕЖНІСТЬ ЗМІЦНЕННЯ 316 АУСТЕНІТНОЇ НЕРЖАВІЮЧОЇ СТАЛІ ПРИ НИЗЬКОТЕМПЕРАТУРНОМУ ОПРОМІНЕННІ ІОНАМИ ІНЕРТНИХ ГАЗІВ

С.О. Карпов, Г.Д. Толстолицька, В.М. Воєводин, Г.М. Толмачова, І.Е. Копанець

Вивчено радіаційно-індуковане зміцнення аустенітної нержавіючої сталі SS316. Зразки опромінювали іонами 1400 кеВ/He і 1400 кеВ/Ar до доз 0,01...10 зсувів на атом (зна) при кімнатній температурі. Зміцнення поверхневого шару досліджували методом наноіндентування. Проаналізовано поведінку кривої твердість–глибина в залежності від сорту іонів. Регресійний аналіз, виконаний для даних по зміцненню з використанням степеневі функції виду $\Delta H \propto (\text{зна})^n$, добре узгоджується з експериментальними даними при $n = 0,47$ і $0,13$ для низькодозного і високодозного режимів зміцнення відповідно. Застосування аналітичної моделі об'ємної частки показало можливість з достатньою точністю моделювати поведінку твердості за глибиною опроміненої нержавіючої сталі.